ACS chemical biology

Articles

pubs.acs.org/acschemicalbiology

Targeting NF-κB p65 with a Helenalin Inspired Bis-electrophile

John C. Widen,[†] Aaron M. Kempema,[†] Peter W. Villalta,[‡] and Daniel A. Harki*[,†,‡]

[†]Department of Medicinal Chemistry and [‡]Masonic Cancer Center, University of Minnesota, 2231 Sixth Street SE, Minneapolis, Minnesota 55455, United States

Supporting Information

ABSTRACT: The canonical NF-κB signaling pathway is a mediator of the cellular inflammatory response and a target for developing therapeutics for multiple human diseases. The furthest downstream proteins in the pathway, the p50/p65 transcription factor heterodimer, have been recalcitrant toward small molecule inhibition despite the substantial number of compounds known to inhibit upstream proteins in the activation pathway. Given the roles of many of these upstream proteins in multiple biochemical pathways, targeting the p50/p65 heterodimer offers an opportunity for enhanced on-target specificity. Toward this end, the p65 protein presents two nondisulfide cysteines, Cys38 and Cys120, at its DNA-binding interface that are amenable to targeting by covalent molecules. The natural product helenalin, a sesquiterpene lactone, has been previously shown to target Cys38 on p65 and ablate its DNA-binding ability. Using helenalin as inspiration, simplified helenalin analogues were designed, synthesized, and shown to inhibit induced canonical NF-κB signaling in cell culture. Moreover, two simplified helenalin probes were proficient at forming covalent protein adducts, binding to Cys38 on recombinant p65, and targeting p65 in HeLa cells without engaging canonical NF-κB signaling proteins IκBα, p50, and IKKα/β. These studies further support that targeting the p65 transcription factor−DNA interface with covalent small molecule inhibitors is a viable approach toward regulating canonical NF-κB signaling.

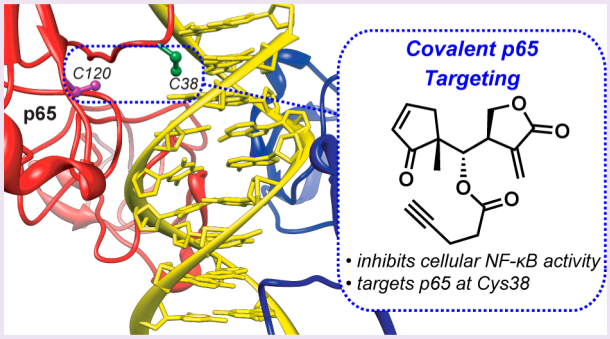

Aberrant activation of canonical p50/p65 NF-κB transcription factors and concomitant expression of their target genes has been implicated in a spectrum of human diseases, including chronic inflammatory disease, atherosclerosis, arthritis, and cancer.[1−4] Consequently, interventional strategies to regulate canonical NF-κB signaling may be broadly useful for multiple therapeutic indications.[5−8] Accordingly, significant research efforts have been devoted toward the discovery of inhibitors of canonical p50/p65 NF-κB signaling with the targeting of upstream kinases that facilitate p50/p65 activation (*via* release from its repressor protein, IκBα) being the prominent strategy.[9,10] However, most of these enzymes have degenerate activities with other cellular processes, and therefore, their inhibition as a strategy to regulate canonical NF-κB signaling results in off-target effects.[9] Targeting the most downstream proteins in the canonical NF-κB signaling pathway, the p50/p65 transcription factor heterodimer itself would ablate such specificity issues.

Chemical modulation of transcription factor−DNA interfaces has shown promise as a strategy to regulate aberrant transcription factor signaling. Pyrrole-imidazole polyamides that target the DNA minor groove with sequence specificity and disrupt transcription factor−DNA binding have demonstrated promising utilities in both cell culture and animal models, including modulation of canonical NF-κB signaling.[11−15] Conversely, targeting transcription factors with protein-binding small molecules has proven more problematic, which has been attributed to the typical shallow ligand binding pockets and nondiscrete protein tertiary structures, which result in weak binding by putative inhibitors.[16,17] Irreversible covalent binding by inhibitors to nucleophilic amino acids on transcription factors may provide another strategy for transcriptional regulation *via* direct protein binding provided the amino acids that are covalently modified are intolerant of chemical modification (e.g., chemical modification prevents DNA binding and/or transcriptional activation).[6]

Many sesquiterpene lactone (SL) natural products are known modulators of NF-κB signaling.[18,19] In particular, helenalin (Figure 1A), an SL isolable from some *Arnica* and *Helenium* species,[20−22] has provided inspiration for the rational design of transcription-factor-targeting NF-κB inhibitors that disrupt DNA binding. The medicinal properties of helenalin have been known for over a century,[23] which are structurally endowed, in part, by its α-methylene-γ-butyrolactone; a moiety found in scores of bioactive natural products.[24] Exocyclic methylene butyrolactones undergo hetero-Michael addition with biological thiols to form covalent adducts. Helenalin also contains an endocyclic α,β-unsaturated ketone (cyclopentenone) that can also undergo hetero-Michael addition with thiols. Removal of one of the two Michael acceptors of helenalin, such as reduction of the cyclopenteone (yielding 2,3-dihydrohelenalin) or α-methylene-γ-butyrolactone (yielding

Received: August 26, 2016
Accepted: November 7, 2016

DOI: 10.1021/acschembio.6b00751
ACS Chem. Biol. XXXX, XXX, XXX−XXX

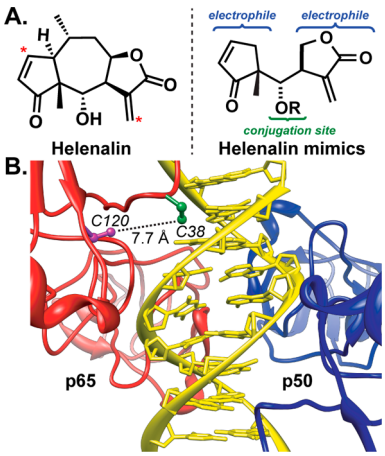

Figure 1. (A) Structure of the sesquiterpene lactone helenalin and the design of helenalin mimics that contain both electrophiles found in the parent natural product. The secondary alcohol is amenable to chemical modifications to install reporter tags, such as alkynes. On the basis of two reported crystal structures of helenalin, the distance between the two electrophilic carbons (red asterisks) is 6.2–6.4 Å.[48,49] (B) X-ray crystal structure of the NF-κB p50–p65 heterodimer bound to DNA (PDB 1VKX).[33] Notably, p65 cysteine residues 38 and 120 are adjacent in the DNA-binding interface (7.7 Å S–S distance, depicted with dashed line).

11,13-dihydrohelenalin; plenolin), significantly diminishes cytotoxicity in comparison to the parent natural product.[25−28] Reduction of both Michael acceptors on helenalin ablates all activity.[26,27] The cyclopentenone and α-methylene-γ-butyrolactone of helenalin can engage biological thiols, such as glutathione and cysteine, yielding covalent adducts.[29,30] Previous studies by Merfort and colleagues have shown that helenalin covalently targets Cys38 of NF-κB p65,[31,32] which is positioned at the DNA-binding interface upon heterodimerization with p50 and DNA engagement (Figure 1B).[33] Alkylation of p65 by helenalin sterically prevents DNA binding of the p50/p65 heterodimer and inhibits its transcriptional activation.[34] Interestingly, molecular modeling of helenalin enabled the hypothesis that it may engage in tandem hetero-Michael additions with Cys38 and Cys120, which are 7.7 Å apart when bound to DNA;[35,36] however, the lack of sensitivity of helenalin to a Cys120 → Ser mutation has drawn this cross-linking model into question.[18,34] Nonetheless, the nondisulfide, nucleophilic cysteines, Cys38 and Cys120, located at the p65 DNA-binding interface constitute unique structural features of p65 that lends itself toward the development of covalent chemical modulators. Furthermore, previous studies from other groups have demonstrated covalent engagement of p65 Cys38 with diverse small molecules,[6,37−41] as well as covalent targeting of p65 Cys120.[42]

We hypothesized that chemical probes containing two structurally similar, α,β-unsaturated carbonyls configured in comparable chemical space to that of helenalin may recapitulate the interesting biological activity of the parent natural product. Consequently, we devised a strategy to develop structurally simplified helenalin analogues that could be amenable to structure–activity relationship studies, serve as suitable chemical mimics of the parent natural product, and yield powerful chemical biology tools for specificity studies and target annotation by protein pulldown-mass spectrometry analysis. Recently, bis-Michael acceptors have been developed to regulate the Keap1/Nrf2/ARE pathway, which supports our approach.[43] Our design would also enable the rapid synthesis of analogues in comparison to helenalin, which required lengthy total syntheses.[44−47] Herein, we report the design, synthesis, and characterization of simplified helenalin analogues and their utilization in cell culture to target p65 of the canonical NF-κB signaling pathway.

RESULTS AND DISCUSSION

Design and Synthesis of Simplified Helenalin Analogues. The probe design was based on retaining both the cyclopentenone and α-methylene-γ-butyrolactone of helenalin, which are required for covalent reactivity at Cys38 and Cys120 of p65, but structurally simplifying the central 7-membered ring, whereas the two above-mentioned ring systems would be tethered in only one position (Figure 1A). In support of this design, computational modeling of **6a** and **6b** predicted distances between the electrophilic carbons (analogous to the electrophilic carbons of helenalin denoted in Figure 1A) on both simplified analogues to be 6.2 Å, which is comparable to those distances measured from published X-ray crystal structures of helenalin (6.2–6.4 Å; see Figure S1 for modeling data).[48,49] Additionally, the calculated distances between the analogous electrophilic carbons on alkynylated probes **1a** and **1b** was similar (**1a**, 6.1 Å; **1b**, 5.4 Å). An additional consideration in our design was the utility of the diastereoselective, Barbier-type, aldehyde allylation chemistry developed by Hodgson and co-workers for synthesizing β-substituted α-methylene-γ-butyrolactones.[50] Accordingly, we devised the five-step racemic synthesis of structurally simplified helenalin probe **6a*** shown in Scheme 1. The known, racemic

Scheme 1. Racemic Synthesis of Bifunctional Helenalin Mimics and Their Alkyne Analogues[a]

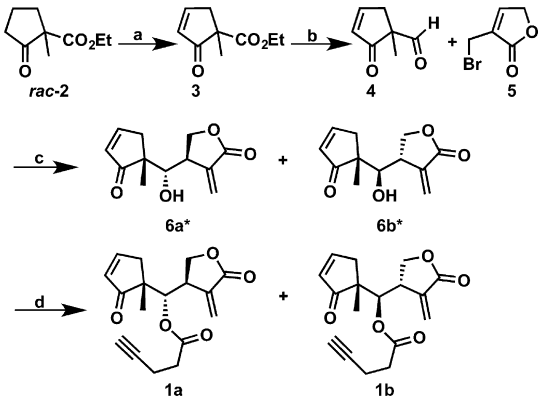

[a]Reagents and conditions: (a) IBX, DMSO, 75 °C, 66%. (b) (i) $LiAlH_4$, Et_2O 0 °C; (ii) PCC, CH_2Cl_2, RT, 40% (two steps). (c) Zn^0, NH_4Cl (aq.), DMF, RT, 60%. (d) 4-Pentynoic acid, DCC, DMAP, CH_2Cl_2, 40 °C, 80% (separable diastereomers). *Denotes **6a** and **6b** prepared from racemic starting materials.

cyclopentanone ***rac*-2**[51−53] was oxidized to the α,β-unsaturated ketone **3** using IBX in moderate yield.[54] β-Keto ester **3** was reduced to the diol with $LiAlH_4$ and then subsequently oxidized to the desired aldehyde **4** with PCC in a 40% yield over the two steps. Notably, aldehyde **4** is volatile and unstable and must be used immediately following careful purification and isolation. The α-(bromo)methyl unsaturated furanone **5** was synthesized in one step from α-methylene-γ-butyrolactone by a known procedure.[50,55] With building blocks **4** and **5** in hand, the

DOI: 10.1021/acschembio.6b00751
ACS Chem. Biol. XXXX, XXX, XXX−XXX

diastereoselective Barbier coupling (*vide supra*) was performed, which resulted in inseparable diastereomers **6a*** and **6b***. Only one diastereomer was observed in the Barbier coupling with respect to β-substitution of the α-methylene-γ-butyrolactone ring in accord with literature precedence of a six-membered transition state. However, metal-catalyzed allylation of aldehyde **4**, bearing a stereogenic center, occurs without facial selectivity, yielding diastereomeric products **6a*** and **6b*** that are racemic. Coupling the inseparable mixture of **6a*** and **6b*** with 4-pentynoic acid and DCC yielded racemic **1a** and **1b** that were separable on silica gel. The overall yield for the synthesis of **1a** and **1b** was 13% (five steps).

A stereoselective synthesis of **6a** was also developed to deliver a simplified helenalin probe with the appropriate overall stereochemistry as that found in helenalin and to overcome our inability to separate diastereomers **6a*** and **6b*** from the Barbier coupling in the racemic synthesis. Since our stereoselective synthesis would employ a different aldehyde coupling partner, an opportunity to separate the diastereomers resulting from the Barbier coupling would exist. Our synthesis began with the stereoselective introduction of the quaternary methyl group, yielding (*S*)-**2**, using an established protocol for the stereoselective methylation of 1,3-ketoesters (Scheme 2).[56−59]

Scheme 2. Enantioselective Synthesis of 6a and 6b[a]

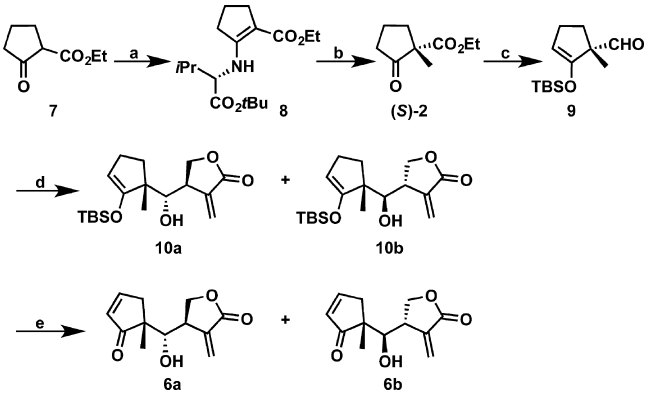

[a]Reagents and conditions: (a) L-Valine *tert*-butyl ester, BF_3·OEt, PhH, reflux (Dean−Stark), 75%. (b) (i) LDA, toluene, THF (2 equiv), −78 °C; MeI; (ii) 3 M HCl (aq.), THF, RT, 53% (2 steps), 93:7 er. (c) (i) LiHMDS, THF; TBSCl, −78 °C to RT; (ii) DIBAL-H, CH_2Cl_2, −78 °C, 27% (2 steps). (d) **5**, Zn^0, NH_4Cl (aq.), DMF, RT, 64% (separable diastereomers). (e) $Pd(OAc)_2$, O_2 (1 atm), DMSO, 46% (**6a**, 93:7 er), 56% (**6b**, 91:9 er).

Accordingly, 1,3-ketoester **7** was condensed with L-*tert*-butylvaline to obtain enamine **8** in 75% yield. Enamine **8** was deprotonated with LDA in toluene at −78 °C, and then two equivalents of THF were added, followed by the addition of excess CH_3I at the same temperature. After formation of the quaternary center, the crude product was isolated, and the resulting Schiff base was hydrolyzed with aqueous HCl to obtain (*S*)-**2** in 53% yield and 93:7 er (85% ee) by chiral-GC analysis. Cyclopentanone (*S*)-**2** was then converted to the TBS-protected enol ether, followed by two-electron reduction of the ester to aldehyde **9** using DIBAL-H in 27% yield (two steps). Notably, addition of the TBS protecting group resulted in a nonvolatile and stable aldehyde **9** in comparison to **4**. Aldehyde **9** was then subjected to the aforementioned Barbier conditions with **5** to obtain diastereomers **10a** and **10b** in 1:1 dr (64% yield) that *were* separable by silica gel chromatography. Diastereomers **10a** and **10b** were oxidized separately to their corresponding cyclopentenones under catalytic Saegusa-Ito oxidation conditions[60,61] in DMSO under 1 atm of O_2 in 46% yield (for **6a**, 93:7 er) and 56% yield (for **6b**, 91:9 er). It is noteworthy that **10a**, **10b**, **6a**, and **6b** should not be dried under high vacuum because of their propensity to decompose (drying under low vacuum for a short period of time is recommended). Enantiomerically pure **6a** and **6b** were synthesized in six steps in 3% and 4% overall yields, respectively.

Stereochemical Determination of Simplified Helenalin Probes. The Barbier coupling utilized for the synthesis of our molecular probes resulted in a highly stereocontrolled β-substitution of the butyrolactone ring. However, the lack of facial selectivity for aldehyde allylation resulted in diastereomers with respect to the quaternary center on the cyclopentanone ring and secondary alcohol. To unambiguously assign the stereochemistry of our probes by X-ray crystallography, we esterified diastereomer **10b** from the enantioselective synthesis with 4-bromobenzoic acid, a moiety that bears a heavy atom for determination of absolute configuration (Scheme 3).

Scheme 3. Synthesis and X-ray Crystal Structure of 11[a]

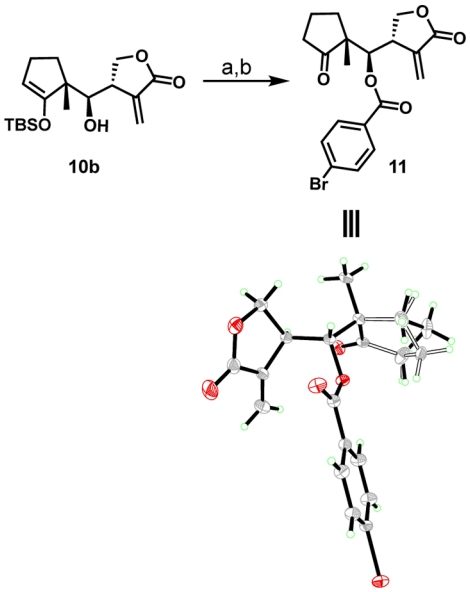

[a]Reagents and conditions: (a) 4-bromobenzoic acid, 4-DMAP, DCC, DCM, 40 °C (99%). (b) TFA, DCM, RT (53%). Bottom: ORTEPII plot of the X-ray diffraction data of **11**.

Deprotection of the silyl enol ether to the ketone using TFA in DCM afforded **11**, which was crystallized and the X-ray structure solved (Supporting Information). On the basis of this information, diagnostic ^{1}H NMR coupling constants, and the known, absolute configuration of (*S*)-**2**, we unambiguously assigned the structures of our chemical probes.

Simplified Helenalin Probes Inhibit NF-κB Signaling in Cell Culture. Simplified helenalin analogues **6a** and **6b** and alkynylated probes **1a** and **1b** were screened for inhibitory activity toward canonical p50/p65 NF-κB signaling with a cellular luciferase assay (Figure 2).[62] Helenalin was utilized as a benchmark and exhibited low micromolar inhibition of induced NF-κB signaling (53.7 ± 14.1% NF-κB activity at 2.5 μM). In comparison, alkyne-functionalized probes **1a** and **1b** were comparably active at 5 μM (54.4 ± 16.7% and 52.9 ± 7.1% NF-

DOI: 10.1021/acschembio.6b00751
ACS Chem. Biol. XXXX, XXX, XXX−XXX

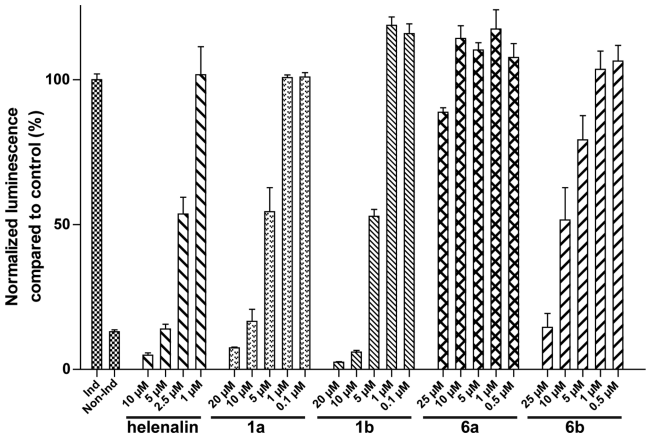

Figure 2. NF-κB-luciferase inhibition assay in A549 cells. Compounds were dosed to A549 cells containing a stably transfected NF-κB luciferase reporter construct and stimulated with TNF-α for 8 h (except for noninduced control, Non-Ind). Luminescence was normalized to the no compound induced (Ind) control and plotted as % NF-κB luciferase activity. Mean ± standard deviation values are shown ($n \geq 3$ biological replicates). Compound-mediated toxicity to A549 cells was measured concurrently (Figure S2).

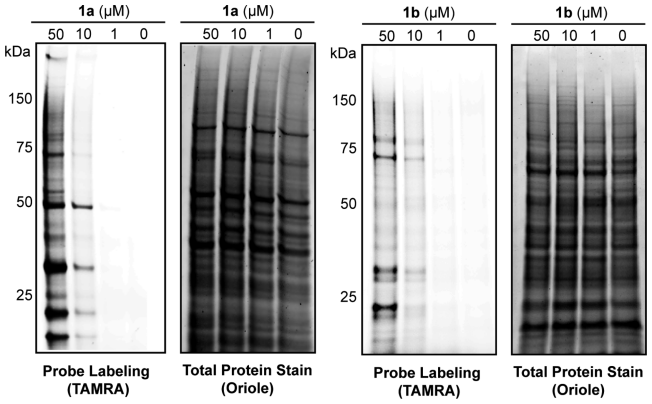

Figure 3. Proteome labeling of **1a** and **1b** in HeLa cells. Compounds were dosed to HeLa cells at the concentrations shown. The cells were lysed, and then TAMRA-N_3 was conjugated to **1a** and **1b** *via* azide–alkyne click chemistry. Proteins were separated by denaturing PAGE, and gels were imaged for TAMRA fluorescence. Total proteins were then visualized by staining with Oriole fluorescent protein stain followed by gel imaging.

κB activity, respectively). Notably, **1a** elicits more cellular cytotoxicity (64.5 ± 3.0% cell viability) during this 8 h assay compared to **1b** (97.8 ± 15.1% cell viability) at 10 μM treatment. Cellular cytotoxicity for **1a** at 20 μM treatment was comparable to that observed at 10 μM, whereas cellular viability was >80% for all other doses of all compounds shown in Figure 2 (refer to Figure S2 for cellular viability data). Intriguingly, enantiomerically pure **6b**, the diastereomer with the "incorrect" stereochemistry with respect to helenalin, has approximately 6-fold more NF-κB inhibitory activity at 25 μM compared to **6a**, the enantiomerically pure "correct" diastereomer from the Barbier coupling (**6b**, 14.5 ± 7.4% NF-κB activity; **6a**, 88.8 ± 4.9% NF-κB activity). Furthermore, **6b** achieves the same NF-κB inhibitory activity as helenalin at only a 4-fold higher dose (**6b**, 51.6 ± 16.6% NF-κB activity at 10 μM; helenalin, 53.7 ± 14.1% NF-κB activity at 2.5 μM). These data suggest the stereochemistries of our helenalin analogues are important with respect to cellular potency. The observation that **1a** and **1b** are equivalently potent in this assay hints at the possibility that **6a** may have poor uptake properties or may be poorly retained in cells; however, no data currently exist to support this proposal.

Simplified Helenalin Probes Covalently Bind Proteins in Cell Culture. To qualitatively assess the protein-binding properties of our probes in cell culture, we performed protein labeling studies in HeLa cells. Alkyne-functionalized **1a** and **1b** were dosed separately to HeLa cells for 1 h, cells were then lysed and the lysate cleared, and then protein-probe adducts were labeled with tetramethylrhodamine-azide (TAMRA-N_3) *via* a copper mediated [3 + 2] Huisgen reaction (click chemistry).[63] Protein-**1a**/**1b**-TAMRA adducts were separated by denaturing PAGE and fluorescence visualization of TAMRA (Figure 3). To demonstrate uniform protein labeling, total proteins were also imaged. Both **1a** and **1b** labeled multiple proteins in a concentration dependent manner (Figure 3). Gratifyingly, protein bands at approximately 65 kDa were observed for both **1a** and **1b**, which would be expected for targeting NF-κB p65. Off-target binding by **1a** and **1b**, which is evident by the multiple protein bands observed in our qualitative analysis, was observed and was certainly anticipated given the designed probes are bis-electrophiles. However, the distinct labeling patterns of **1a** and **1b** further reinforce the relevance of the stereochemistry of our probes with respect to protein targeting. Probe **1a** (which contains the correct stereochemistry with respect to helenalin) qualitatively labels more proteins compared to **1b** by visualization of the intense bands seen at 50 and 10 μM. Additionally, pretreatment of cells with helenalin prior to labeling studies with **1a** competes away protein binding properties by **1a**, suggesting that our designed probe mimics the proteome reactivity properties of the parent natural product (Figure S3).

Helenalin and Simplified Helenalin Probes Covalently Label Cys38 of Recombinant p65. Previous studies with wild-type p65 and Cys → Ser mutant p65 proteins have demonstrated that helenalin covalently targets Cys38.[34] To evaluate if helenalin mimics **1a** and **1b** also target Cys38, recombinant human p65 was incubated with **1a** and **1b**, proteins were digested, and LC-MS/MS was performed to identify adducted thiols (Figure 4). The predicted trypsin digestion of p65 proximal to Cys38 yields $C^{38}EGR^{41}$ or $Y^{36}KCEGR^{41}$ if the cleavage site closest to Cys38 is missed. Searching for the exact masses of the probes as a cysteine modification found the expected probe-peptide adducts for helenalin ($Y^{36}KCEGR^{41}$ adduct), **1a** ($C^{38}EGR^{41}$ adduct) and **1b** ($C^{38}EGR^{41}$ adduct). Analysis of the MS^2 data for studies with **1a** and **1b** and recombinant p65 consistently revealed a fragment that was cleaved at the secondary hydroxyl group, which demonstrates that the α-methylene-γ-butyrolactone was reacting with Cys38 (Figure 4 and Figures S4–S5). On the other hand, no fragments were found to support reactivity at the endocyclic enones of **1a** and **1b**, although such adducts might be reversible and unstable to digestion and MS analysis. Our reactivity data are consistent with previous reports demonstrating that α-methylene-γ-butyrolactones form irreversible hetero-Michael addition adducts with cysteines.[30,31] Interestingly, attempts to identify Cys38 adducts for **6a** and **6b** were unsuccessful, although adducts to a surface cysteine on p65, Cys105, was observed (Figure S7). Cys105 adducts were not found in experiments with **1a**, **1b**, or helenalin. The biological significance of labeling Cys105 on p65 remains unclear.

DOI: 10.1021/acschembio.6b00751
ACS Chem. Biol. XXXX, XXX, XXX–XXX

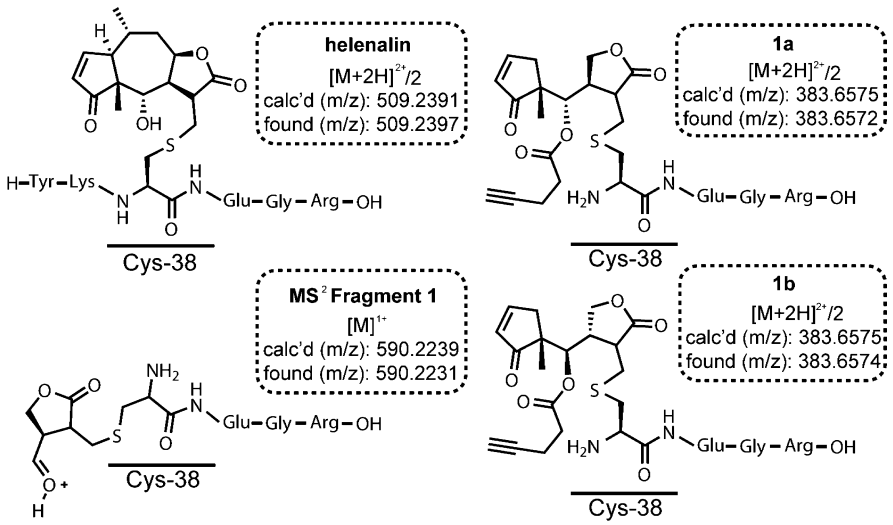

Figure 4. Annotation of compound binding sites on p65. Helenalin, **1a**, and **1b** were incubated separately with recombinant human p65 in 1 × PBS buffer for 1 h. Proteins were digested with trypsin and peptides analyzed by LC-MS/MS. Peptide-probe adducts were identified by extracting the theoretical mass from the total ion chromatogram and then analysis of the MS^2 fragmentation pattern. Helenalin, **1a**, and **1b** all bound Cys38 as expected. The MS^2 Fragment 1 (shown on the bottom left) was detected after dosing **1a** and **1b**, indicating that covalent adducts are forming at the exocyclic methylene butyrolactone.

Simplified Helenalin Probes Covalently Target p65 in Cell Culture. After determining that simplified helenalin probes **1a** and **1b** can inhibit canonical NF-κB signaling in cell culture, covalently label cellular proteins, and target Cys38 of recombinant p65, we turned our attention to evaluating whether **1a** and **1b** can directly bind p65 in cell culture and avoid other well-established canonical NF-κB signaling enzymes. Accordingly, **1a** and **1b** were dosed to HeLa cells at 50 μM and incubated for 30 min. Cells were then harvested, washed extensively to remove unincorporated probe, and then lysed by sonication. Protein-**1a**/**1b** adducts were then labeled with biotin-azide (biotin-N_3) *via* a copper mediated [3 + 2] Huisgen reaction (click chemistry).[63] Protein-**1a**/**1b**-biotin adducts were enriched with a monomeric avidin column and separated by denaturing PAGE. Protein-**1a**/**1b**-biotin adducts were transferred to a membrane and then incubated with primary antibodies for p65 (primary target), IκBα (p50/p65 repressor protein; for specificity assessment), p50 (forms transcription factor heterodimer with p65; for specificity assessment), and IKKα/β (upstream kinases that contribute to activation of the NF-κB signaling pathway; for specificity assessment; antibody recognizes both proteins). To our delight, simplified helenalin probes **1a** and **1b** successfully pulled down p65 from live HeLa cells but did not target IκBα, p50, or IKKα/β (Figure 5). The negative control demonstrates no proteins are pulled down in the absence of probes, and the input lysates show that all proteins being evaluated are present in the input lysate (prior to monomeric avidin isolation of protein-**1a**/**1b**-biotin adducts). Furthermore, a head-to-head comparison of the ability of **1a** and **1b** to target p65 reveals comparable efficiencies (Figure 5C).

We also wanted to determine if **6a** and **6b** could compete away binding of alkyne probes **1a** and **1b** in live cells; especially since p65 adducts were not observed with **6a** and **6b** by MS analysis. To this end, **6a** and **6b** were dosed to HeLa cells at 50 μM for 20 min prior to dosing **1a** or **1b**. Interestingly, **6b** was able to completely block labeling and pulldown by both **1a** and **1b**, whereas **6a** exhibited only partial activity at the same concentration (Figure 5). These data suggest that **6a** and **6b** target Cys38 on p65. Additionally, the difference in efficiencies between the two compounds is consistent with the cellular reporter data (Figure 2), in which **6a** was dramatically less potent than **6b** for inhibition of canonical NF-κB signaling.

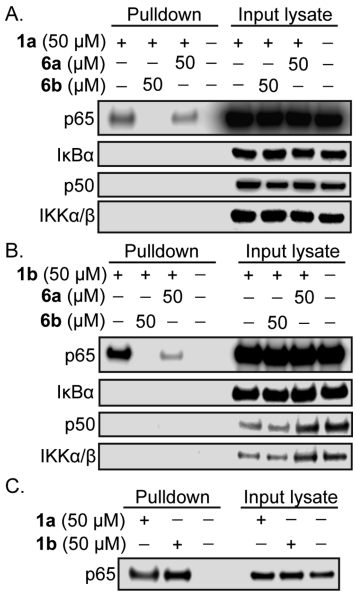

Figure 5. Immunodetection of NF-κB signaling pathway proteins for covalent binding by **1a** and **1b**. Compounds were dosed to HeLa cells at the concentrations shown, the cells were lysed, and then Biotin-N_3 was conjugated to **1a** and **1b** *via* azide−alkyne click chemistry. Protein-**1a**/**1b** adducts were isolated on monomeric avidin resin and identified by Western blotting with the antibodies shown. Notably, IKKα/β is recognized with the same antibody. (A, B) **1a** (for A) and **1b** (for B) label p65 but not other NF-κB pathway proteins, as shown in pulldown experiments. Competition experiments were performed by pretreating cells with **6a** and **6b** 20 min before the addition of **1a** (for A) or **1b** (for B). (C) Head-to-head comparison of labeling efficiency of **1a** and **1b**. Input lysate is the crude protein product before monomeric avidin enrichment.

DOI: 10.1021/acschembio.6b00751
ACS Chem. Biol. XXXX, XXX, XXX−XXX

Conclusions. We have developed simplified helenalin probes that target Cys38 of NF-κB p65 by a covalent mechanism of action. Our chemical probes are easily accessed in six synthetic steps (to probes **1a** and **1b**) and contain an alkyne handle for imaging and protein pulldown applications. Simplified helenalin probes **1a** and **1b** inhibit induced, canonical NF-κB signaling in a cellular reporter assay with low micromolar efficiencies and selectively engage p65 over other well-established proteins whose targeting by small molecules affects canonical NF-κB signaling, namely, IκBα, p50, and IKKα/β. The strategy of covalent targeting of solvent accessible, nucleophilic amino acids at key transcription factor interfaces, such as the DNA-binding cleft for p65 in this work, represents a viable strategy to rationally design small molecule transcription factor binders with biochemical utilities for transcriptional control of aberrant gene expression in human diseases. Current efforts are focused on improving the specificities and potencies of the first-generation helenalin-based probes reported in this work, with a particular focus on the size and rigidity of the moieties that mimic the central seven-membered ring of helenalin.

■ MATERIALS AND METHODS

Materials and Synthetic Methods. Unless otherwise noted, reactions were performed in flame-dried glassware under a nitrogen or argon atmosphere and stirred with a Teflon-coated magnetic stir bar. Liquid reagents and solvents were transferred *via* syringe and cannula using standard techniques. Reaction solvents dichloromethane (DCM), N,N-dimethylformamide (DMF), tetrahydrofuran (THF), and diethyl ether (Et_2O) were dried by passage over a column of activated alumina using a solvent purification system (MBraun). All other chemicals were used as received unless otherwise noted. Helenalin was purchased from Enzo Life Sciences and purified by SiO_2 flash column chromatography before use in biological assays. The molarities of *n*-butyllithium solutions were determined by titration against diphenylacetic acid as an indicator (average of three determinations). Reaction temperatures above 23 °C refer to oil bath temperature, which was controlled by a temperature modulator. Reaction progress was monitored by thin layer chromatography using EMD Chemicals Silica Gel 60 F_{254} glass plates (250 μm thickness) and visualized by UV irradiation (at 254 nm) and/or $KMnO_4$ stain. Silica gel chromatography was performed on a Teledyne-Isco Combiflash Rf-200 instrument utilizing Redisep Rf High Performance silica gel columns (Teledyne-Isco), or flash column chromatography was performed using SiliCycle silica gel (32−63 μm particle size, 60 Å pore size). ^{1}H NMR (500 MHz), ^{13}C NMR (125 MHz), and ^{19}F NMR (470 MHz) spectra were recorded on a Bruker Avance NMR spectrometer. ^{1}H and ^{13}C chemical shifts (δ) are reported relative to the solvent signal, $CHCl_3$ (δ = 7.26 for ^{1}H NMR and δ = 77.00 for ^{13}C NMR). Some spectra contain TMS (0.05% v/v). All NMR spectra were obtained at RT unless otherwise specified. High resolution mass spectral data were obtained at the Analytical Biochemistry Core Facility of the University of Minnesota Masonic Cancer Center on an LTQ Orbitrap Velos Mass Spectrometer (Thermo Fisher).

The purities of all compounds tested in biological assays were checked *via* analytical HPLC analysis on an Agilent 1200 series instrument equipped with a diode array detector (wavelength monitored = 215 nm) and a Zorbax SBC18 column (4.6 × 150 mm, 5.0 μm, Agilent Technologies). All compounds tested in biological assays were >95% pure by HPLC. Information regarding the HPLC method and purity traces can be found in the Supporting Information.

The enantiopurity of (*S*)-**2** was determined by chiral-GC/MS using an Agilent 7200B GC/Q-TOF with an Agilent J&W CycloSil-B GC column (30 m × 0.25 mm, 0.25 μm film). The injector port was set at 250 °C and the column flow (helium gas) at 1.0 mL/min. The temperature method began at 35 °C and increased to 180 °C (8 °C/min) over 18.1 min. The mass spectrometer electron ionization source temperature was set to 250 °C for detection. Area under the peak for each enantiomer was used to determine the enantiopurity, reported as enantiomeric ratio (er). The enantiopurity of other compounds was determined using normal phase chiral-HPLC or ^{19}F analysis after derivatization with (*S*)-(−)-α-methoxy-α-(trifluoromethyl)-phenylacetic acid ((S)-MTPA). Information regarding these two methods can be found in the Supporting Information.

*Ethyl 1-Methyl-2-oxocyclopent-3-enecarboxylate (**3**).*[51−53] To a stirred solution of ***rac*-2** (1.00 g, 5.88 mmol) in DMSO (20 mL) was added 4.11 g (14.7 mmol) of IBX,[64] and the solution was heated to 85 °C for 18 h. The reaction was cooled to 0 °C, and aqueous $NaHCO_3$ (saturated, 40 mL) was added slowly. The reaction was filtered to remove IBX decomposition products. The solution was extracted with Et_2O (30 mL, 3×), and the organic layer was dried over Na_2SO_4 and concentrated *in vacuo*. The crude mixture was SiO_2 purified with EtOAc (10−30%) in hexanes to afford **3** (0.52 g, 53% yield) as a slightly tinted yellow oil. ^{1}H NMR ($CDCl_3$): 7.76−7.71 (m, 1H), 6.19−6.15 (m, 1 H), 4.14 (q, *J* = 7.2 Hz, 2 H), 3.25 (d, *J* = 19.1 Hz, 1 H), 2.53 (d, *J* = 19.2 Hz, 1 H), 1.39 (s, 3H), 1.21 (t, *J* = 7.2 Hz, 3H) ppm. ^{13}C NMR ($CDCl_3$): 206.9, 171.7, 163.2, 131.8, 61.7, 53.5, 42.9, 20.8, 14.2 ppm. HRMS-ESI$^+$ (*m*/*z*) calcd [M + H]$^+$ for $C_9H_{12}O_3$: 169.0859. Found: 169.0855.

5-(Hydroxymethyl)-5-methylcyclopent-2-enol. To a stirred suspension of $LiAlH_4$ (0.66 g, 17 mmol) in EtO_2 (25 mL) at 0 °C was added **3** (0.75 g, 4.4 mmol) in EtO_2 (6 mL) dropwise. The reaction was stirred at 0 °C for 2 h. The reaction was carefully quenched with H_2O (1 mL), then aqueous NaOH (10%, 0.5 mL), and finally H_2O (2 mL) and stirred overnight. The reaction was then filtered through Celite, and the filtrate was concentrated *in vacuo*. The crude mixture was SiO_2 purified with EtOAc (30−100%) in hexanes to afford a clear oil (0.46 g, 80% yield). ^{1}H NMR analysis was consistent with that reported previously.[65−67]

*1-Methyl-2-oxocyclopent-3-enecarbaldehyde (**4**).* The diol product (0.31 g, 2.3 mmol) from above was dissolved in DCM (20 mL) at RT and stirred. PCC (1.51 g, 7.03 mmol) was added in 3 equiv portions over 4 h while stirring. This reaction was not kept under an inert atmosphere. The reaction was vacuum filtered through Celite. The resulting solution was carefully concentrated on a rotary evaporator (no water bath; 150 Torr vacuum) until only a small amount of solution remained. This solution was introduced onto a silica column (1 in. diameter, 4 in. length) and quickly purified (10% Et_2O in pentanes). The fractions containing the desired compound were collected and concentrated carefully (as described above) to afford a volatile, clear oil **4** (0.16 g, 55% yield). *Note: Concentration until no residual solvent is left will result in loss of product and decreased yields. Do not use a high vacuum to dry product. After isolation, the product was used immediately in the next reaction. If stored at −20 °C in DCM, the compound degrades in the span of 24 h.* ^{1}H NMR ($CDCl_3$): 9.43 (s, 1H), 7.82−7.77 (m, 1H), 6.16−6.12 (m, 1H), 3.37 (dt, *J* = 19.4, 2.5 Hz, 1H), 2.41 (dt, *J* = 19.4, 2.3 Hz, 1H), 1.45 (s, 3H) ppm. ^{13}C NMR ($CDCl_3$): 206.0, 198.1, 164.4, 132.0, 60.6, 37.4, 18.2 ppm. HRMS-ESI$^+$ (*m*/*z*) calcd [M + H]$^+$ for $C_7H_8O_2$: 125.0597. Found: 125.0594.

*Rac-(R)-4-((S)-Hydroxy((R)-1-methyl-2-oxocyclopent-3-en-1-yl)-methyl)-3-methylenedihydrofuran-2(3H)-one (**6a***) *and rac-(S)-4-((R)-Hydroxy((R)-1-methyl-2-oxocyclopent-3-en-1-yl)methyl)-3-methylenedihydrofuran-2(3H)-one (**6b***).* Compounds **4** (69 mg, 0.56 mmol) and **5**[50,55] (55 mg, 0.84 mmol) were combined in a round-bottom flask containing DMF (3 mL) and a stir bar. Activated Zn^0 (109 mg, 1.68 mmol) was added to the stirring solution. Zn^0 was freshly activated before each reaction by stirring in aqueous HCl (4 M) for 15 min and then filtered; washed with H_2O (200 mL, 3×), MeOH (200 mL), EtOAc (200 mL), and Et_2O (100 mL); and dried under a high vacuum for at least 1 h. Aqueous NH_4Cl (saturated, 1 drop) was added to the solution. The reaction was degassed and backfilled with Ar(g) 3× and then allowed to stir at RT for 16 h. The reaction was quenched with H_2O (15 mL) and extracted with Et_2O (20 mL, 3×), then dried over Na_2SO_4 and concentrated *in vacuo* to a crude oil. The crude oil was SiO_2 purified with EtOAc (0 to 70%) in hexanes to give

DOI: 10.1021/acschembio.6b00751
ACS Chem. Biol. XXXX, XXX, XXX−XXX

74 mg (60% yield) of a clear oil containing **6a*** and **6b*** that was an inseparable mixture of diastereomers. The NMR characterization data for the separated, enantiomerically enriched compounds are below. See the Supporting Information for methodology used for enantiopurity analysis of synthesized compounds. For **6a***, a modest chiral induction was observed in the Barbier coupling reaction in a 32:68 dr for the resulting esterified, (S)-MTPA analogues by ^{19}F NMR. For **6b***, no chiral induction was observed, as evidenced by the 1:1 er by chiral-HPLC analysis.

*Rac-(S)-((R)-1-Methyl-2-oxocyclopent-3-en-1-yl)((R)-4-methylene-5-oxotetrahydrofuran-3-yl)methyl pent-4-ynoate (**1a**) and rac-(R)-((R)-1-Methyl-2-oxocyclopent-3-en-1-yl)((S)-4-methylene-5-oxotetrahydrofuran-3-yl)methyl pent-4-ynoate (**1b**).* The previously isolated mixture of **6a*** and **6b*** (14 mg, 0.06 mmol) were dissolved in DCM (5 mL); then 4-pentynoic acid (12 mg, 0.13 mmol) was added to this solution. 4-DMAP (31 mg, 0.25 mmol) was then added followed by DCC (39 mg, 0.19 mmol). The reaction was heated to 40 °C for 4 h. The reaction was quenched with H_2O (5 mL) and extracted with DCM (10 mL, 3×). The organic layer was dried over Na_2SO_4, filtered, and concentrated *in vacuo* to afford a crude oil. The crude product was SiO_2 purified with EtOAc (0−70%) in hexanes to afford two white solids with an overall yield of 15 mg (80% yield, 1:1 ratio of **1a**/**1b**).

1a. ^{1}H NMR ($CDCl_3$): 7.73−7.68 (m, 1H), 6.38 (s, 1H), 6.19−6.14 (m, 1H), 5.72 (s, 1H), 5.17 (d, J = 4.9 Hz, 1H), 4.36 (dd, J = 9.5, 7.6 1H), 4.27 (dd, J = 9.6, 2.8 Hz, 1H), 3.60−3.52 (m, 1H), 2.97 (dt, J = 19.0, 2.4 Hz, 1H), 2.49−2.33 (m, 5H), 1.95 (t, J = 2.3 Hz, 1H), 1.20 (s, 3H) ppm. ^{13}C NMR ($CDCl_3$): 210.1, 170.4, 169.8, 163.2, 134.5, 132.0, 125.4, 82.0, 77.0, 69.9, 69.3, 49.8, 40.8, 40.2, 33.2, 20.3, 14.1 ppm. HRMS-ESI$^+$ (m/z) calcd [M + H]$^+$ for $C_{18}H_{20}O_3$: 303.1227. Found: 303.1222.

1b. ^{1}H NMR ($CDCl_3$): 7.76−7.72 (m, 1H), 6.28 (s, 1H), 6.26−6.20 (m, 1H), 5.56 (s, 1H), 5.10 (d, J = 6.3 Hz, 1H), 4.30−4.27 (m, 2H), 3.56−3.50 (m, 1H), 2.92 (dt, J = 19.8, 2.4 Hz, 1H), 2.54−2.42 (m, 5H), 1.98 (t, J = 2.4 Hz, 1H), 1.19 (s, 3H) ppm. ^{13}C NMR ($CDCl_3$): 209.8, 169.9, 168.8, 162.4, 133.5, 132.4, 124.3, 81.0, 76.8, 69.0, 68.5, 48.4, 40.2, 38.5, 32.4, 21.6, 13.2 ppm. HRMS-ESI$^+$ (m/z) calcd [M + H]$^+$ for $C_{18}H_{20}O_3$: 303.1227. Found: 303.1222.

*(S)-2-((1-(tert-Butoxy)-3-methyl-1-oxobutan-2-yl)amino)-cyclopent-1-ene-1-carboxylate (**8**).* The synthetic procedure was adapted from that previously reported.[56−59] To remove the salt of L-valine *tert*-butyl ester hydrochloride, the material was dissolved in EtOAc (100 mL), and aqueous NaOH (0.5 M, 100 mL) was added and stirred for 10 min. The material was extracted with EtOAc (100 mL, 3×), washed with brine (15 mL, 1×), dried over Na_2SO_4, concentrated *in vacuo* to a clear oil, and then immediately used. To a stirred solution of **7** (2.99 g, 19.1 mmol) and L-valine *tert*-butyl ester (4.31 g, 24.9 mmol) in benzene (50 mL) was added $BF_3{\cdot}OEt_2$ (1.18 mL, 9.55 mmol). The reaction mixture was refluxed with a Dean−Stark trap for 24 h. The reaction was allowed to cool to RT and quenched with aqueous $NaHCO_3$ (saturated, 50 mL) and then extracted with Et_2O (50 mL, 3×), washed with brine (10 mL, 1×), and dried over Na_2SO_4. The organic layer was concentrated *in vacuo*. The crude product was SiO_2 purified with EtOAc (0−5%) in hexanes to afford **8** (4.46 g, 75%) as a white solid. ^{1}H NMR (500 MHz): 7.63 (bs, 1H), 4.22−2.11 (m, 2H), 3.64 (dd, J = 10.0, 5.5 Hz, 1H), 2.52 (t, J = 7.1 Hz, 2H), 2.47 (t, J = 7.6 Hz, 2H), 2.17−2.06 (m, 1H), 1.81 (p, J = 7.4 Hz, 2H), 1.46 (s, 9H), 1.27 (t, J = 7.1 Hz, 3H), 0.98 (app t, 6H) ppm. ^{13}C NMR (125 MHz): 171.3, 168.2, 163.1, 94.7, 81.6, 63.9, 58.6, 32.3, 31.8, 29.3, 28.0, 20.9, 19.2, 17.8, 14.8. HRMS-ESI$^+$ (m/z) calcd [M + H]$^+$ for $C_{17}H_{29}NO_4$: 312.2169. Found: 312.2163.

*Ethyl (S)-1-Methyl-2-oxocyclopentane-1-carboxylate ((S)-**2**).* Stereoselective methylation was adapted from that previously reported.[56−59] *n*-BuLi in hexanes (2.0 M solution, 3.56 mL, 7.13 mmol) was added to a solution of DIPA (1.00 mL, 7.13 mmol) at −78 °C in anhydrous toluene (30 mL), and the reaction was warmed to 0 °C and stirred for 30 min. The reaction mixture was cooled to −78 °C, and **8** (1.85 g, 5.94 mmol) in anhydrous toluene (10 mL) was added dropwise and stirred for 1 h. THF (0.96 mL, 11 mmol) was added to the reaction and stirred for 2 h. MeI (1.85 mL, 29.7 mmol) was added, and the reaction was stirred at −78 °C for 16 h. The reaction was then quenched with aqueous NH_4Cl (saturated, 50 mL) and extracted with Et_2O (30 mL, 3×), washed with brine (15 mL, 1×), dried over Na_2SO_4, and concentrated *in vacuo*. The crude products were then dissolved in THF (50 mL), and aqueous HCl (3M, 50 mL) was added and stirred at RT for 6 h. The reaction was extracted with Et_2O (50 mL, 3×), washed with water (10 mL, 1×) and then brine (15 mL, 1×), and dried over Na_2SO_4. The solvent was concentrated *in vacuo*. The crude mixture was SiO_2 purified with EtOAc (0%−20%) in hexanes to afford (S)-**2** as a colorless oil (0.54 g, 53%, 93:7 er by chiral-GCMS). NMR characterization was consistent with previously reported data for this compound.[51]

Ethyl (S)-2-((tert-Butyldimethylsilyl)oxy)-1-methylcyclopent-2-ene-1-carboxylate. LiHMDS solution in THF (1 M solution, 4.20 mL, 4.19 mmol) was added to anhydrous THF (30 mL) at −78 °C. Next, a solution of **9** (0.59 g, 3.5 mmol) in THF (5 mL) was added dropwise and stirred for 1 h at −78 °C. A solution of TBSCl (1.05 g, 6.98 mmol) in THF (10 mL) was then added dropwise at −78 °C, and then the reaction was allowed to slowly come to RT and stirred for 16 h. The reaction mixture was quenched with aqueous NH_4Cl (saturated, 30 mL) and extracted with Et_2O (30 mL, 3×). The organic layer was washed with brine (15 mL, 1×), dried over Na_2SO_4, and concentrated *in vacuo*. The crude material was SiO_2 purified with EtOAc (0 to 10%) in hexanes, resulting in a clear oil (0.78 g, 79% yield). ^{1}H NMR (500 MHz): 4.61 (t, J = 2.2 Hz, 1H), 4.12 (q, J = 7.2 Hz, 2H), 2.40−2.29 (m, 2H), 2.29−2.19 (m, 1H), 1.77−1.67 (m, 1H), 1.72 (m, 1H), 1.30 (s, 3H), 1.24 (t, J = 7.1 Hz, 3H), 0.90 (s, 9H), 0.16 (s, 3H), 0.15 (s, 3H). ^{13}C NMR (125 MHz): 176.1, 156.2, 101.2, 60.5, 54.3, 35.3, 26.2, 25.5, 21.3, 18.0, 14.2, −5.0, −5.2 ppm. HRMS-ESI$^+$ (m/z) calcd [M + H]$^+$ for $C_{15}H_{28}O_3Si$: 285.1881. Found: 285.1883.

*(S)-2-((tert-Butyldimethylsilyl)oxy)-1-methylcyclopent-2-enecarbaldehyde (**9**).* To a solution of anhydrous DCM (20 mL) was added the silyl enol ether from the above reaction (0.91 g, 3.19 mmol), and the resulting solution was cooled to −78 °C. A solution of DIBAL-H in DCM (1M, 3.19 mL, 3.19 mmol) was added dropwise to the reaction mixture and stirred for 4 h at −78 °C. The reaction was then carefully quenched with H_2O (1 mL); aqueous NaOH (0.5M, ∼ 0.1 mL) was added and then an additional aliquot of H_2O (1 mL). The reaction was gravity filtered through qualitative filter paper, washed with brine (10 mL, 1×), dried over Na_2SO_4, and concentrated *in vacuo*. The crude product was SiO_2 purified with EtOAc (0−5%) in hexanes to afford a clear oil (0.29 g, 38% yield). ^{1}H NMR (500 MHz): 9.53 (s, 1H), 4.75 (t, J = 2.3 Hz, 1H), 2.34−2.25 (m, 3H), 1.72−1.60 (m, 1H), 1.20 (s, 3H), 0.90 (s, 9H), 0.17 (s, 3H), 0.15 (s, 3H) ppm. ^{13}C NMR (125 MHz): 202.5, 154.2, 103.2, 59.3, 30.7, 26.0, 25.5, 18.0, 17.6, −4.9, −5.0; impurities at 25.7, −3.6 ppm. HRMS-ESI$^+$ (m/z) calcd [M + H]$^+$ for $C_{13}H_{24}O_2Si$: 241.1618. Found: 241.1616.

*(R)-4-((S)-((R)-2-((tert-Butyldimethylsilyl)oxy)-1-methylcyclopent-2-en-1-yl)(hydroxy)methyl)-3-methylenedihydrofuran-2(3H)-one (**10a**) and (S)-4-((R)-((R)-2-((tert-Butyldimethylsilyl)oxy)-1-methylcyclopent-2-en-1-yl)(hydroxy)methyl)-3-methylenedihydrofuran-2(3H)-one (**10b**).* To a solution of DMF (3 mL), **9** (0.29 g, 1.2 mmol), and **5**[50,55] (0.32 g, 1.8 mmol) was added powdered Zn^0 (0.32 g, 4.8 mmol, activated as described for **6a***/**6b***). Aqueous NH_4Cl (saturated, one drop) was added, and the reaction was degassed and backfilled with Ar(g) (3×). The reaction was then stirred at RT for 16 h. The reaction mixture was quenched with H_2O (15 mL) and extracted with Et_2O (15 mL, 3×). The organic layer was washed with H_2O (10 mL, 1×) and then brine (10 mL, 1×). The subsequent organic layer was dried over Na_2SO_4 and concentrated *in vacuo*. The crude mixture was SiO_2 purified with an isocratic eluent system EtOAc (20%) in hexanes to afford the separated diastereomers **10a** and **10b** as white solids (0.41 g, 64% yield, 1:1 dr). *Note: **10a**/**10b** will polymerize when concentrated, and/or the silyl enol ether will be deprotected if allowed to sit at RT as a solid for an extended period of time. To avoid this, do not dry under a high vacuum, and after concentration with a low vacuum pump immediately take **10a** and **10b** on to the next reaction.*

10a. ^{1}H NMR (500 MHz): 6.42 (d, J = 1.6 Hz, 1H), 5.91 (d, J = 1.0 Hz, 1H), 4.66 (t, J = 2.4 Hz, 1H), 4.22 (dd, J = 9.2, 4.1 Hz, 1H), 4.22 (dd, J = 9.2, 4.1 Hz, 1H), 3.62 (dd, J = 6.6, 4.1 Hz, 1H), 3.29−3.22 (m,

DOI: 10.1021/acschembio.6b00751
ACS Chem. Biol. XXXX, XXX, XXX−XXX

1H), 2.27−2.19 (m, 2H), 2.17−2.08 (m, 1H), 2.0 (d, J = 4.2 Hz, 1H), 1.62−1.51 (m, 1H), 1.10 (s, 3H), 0.93 (s, 9H), 0.20 (s, 3H), 0.17 (s, 3H) ppm. ^{13}C NMR (125 MHz): 170.8, 156.9, 135.0, 126.2, 102.0, 76.1, 70.3, 51.9, 41.3, 31.1, 25.7, 25.4, 21.8, 18.0, −4.6, −5.3 ppm. HRMS-ESI$^+$ (m/z) calcd [M + H]$^+$ for $C_{18}H_{30}O_4Si$: 339.1986. Found: 339.1982.

10b. ^{1}H NMR (500 MHz): 6.40 (d, J = 1.1 Hz, 1H), 6.01 (s, 1H), 4.62 (t, J = 2.3 Hz, 1H), 4.24 (dd, J = 9.4, 3.1 Hz, 1H), 4.24 (dd, J = 9.4, 5.3 Hz, 1H), 3.64 (dd, J = 8.6, 3.7 Hz, 1H), 3.23−3.16 (m, 1H), 2.51 (d, J = 3.7 Hz, 1H), 2.30−2.12 (m, 2H), 2.07−1.99 (m, 1H), 1.63−1.55 (m, 1H), 1.20 (s, 3H), 0.94 (s, 9H), 0.22 (s, 3H), 0.18 (s, 3H) ppm. ^{13}C NMR: 170.9, 157.4, 135.7, 126.0, 101.9, 77.4, 68.9, 51.3, 42.4, 30.7, 25.8, 25.6, 22.7, 18.0, −4.4, −5.5 (125 MHz). HRMS-ESI$^+$ (m/z) calcd [M + H]$^+$ for $C_{18}H_{30}O_4Si$: 339.1986. Found: 339.1978.

*(R)-4-((S)-Hydroxy((R)-1-methyl-2-oxocyclopent-3-en-1-yl)-methyl)-3-methylenedihydrofuran-2(3H)-one (**6a**).* Compound **10a** (22 mg, 0.074 mmol) was dissolved in DMSO (2 mL), and $Pd(OAc)_2$ (7.0 mg, 0.013 mmol) was added. The reaction was placed under 1 atm of O_2 (g) and stirred at RT for 24 h. The reaction mixture was quenched with H_2O (10 mL) and extracted with Et_2O (15 mL, 3×). The organic layer was washed with H_2O (10 mL, 1×) and then brine (10 mL, 1×), dried over Na_2SO_4, and concentrated *in vacuo*. The crude mixture was SiO_2 purified with EtOAc (0−80%) in hexanes to afford **6a** (10 mg, 46% yield, 93:7 er), as a clear oil. ^{1}H NMR (500 MHz): 7.78−7.72 (m, 1H), 6.46 (d, J = 2.1 Hz, 1H), 6.20−6.16 (m, 1H), 5.81 (d, J = 1.9 Hz, 1H), 4.43 (dd, J = 9.4, 7.7 Hz, 1H), 4.24 (dd, J = 9.4, 3.1 Hz, 1H), 3.97 (d, J = 5.7 Hz, 1H), 3.35−3.29 (m, 1H), 3.10 (app dt, J = 18.9, 2.5 Hz, 1H), 2.35 (app dt, J = 18.9, 2.8 Hz, 1H), 1.14 (s, 3H) ppm. ^{13}C NMR (125 MHz): 213.0, 170.3, 164.3, 134.6, 132.0, 126.3, 75.9, 69.9, 51.4, 41.4, 39.5, 21.1 ppm. HRMS-ESI$^+$ (m/z) calcd [M + H]$^+$ for $C_{12}H_{14}O_4$: 223.0965. Found: 223.0963.

*(S)-4-((R)-Hydroxy((R)-1-methyl-2-oxocyclopent-3-en-1-yl)-methyl)-3-methylenedihydrofuran-2(3H)-one (**6b**).* Compound **10b** (12 mg, 0.04 mmol) was dissolved in DMSO (2 mL), and $Pd(OAc)_2$ (1.00 mg, 0.004 mmol) was added. The reaction was placed under 1 atm of O_2(g) and stirred at RT for 24 h. The reaction mixture was quenched with H_2O (10 mL) and extracted with Et_2O (15 mL, 3×). The organic layer was washed with H_2O (10 mL, 1×) and then brine (10 mL, 1×). The subsequent organic layer was dried over Na_2SO_4 and concentrated *in vacuo*. The crude mixture was SiO_2 purified with EtOAc (0−80%) in hexanes to afford **6b** (4.0 mg, 56% yield, 91:9 er) as a clear oil. ^{1}H NMR (500 MHz): 7.77−7.73 (m, 1H), 6.39 (d, J = 2.7 Hz, 1H), 6.24−6.16 (m, 1H), 5.98 (d, J = 2.3 Hz, 1H), 4.32−4.23 (m, 1H), 4.15 (dd, J = 9.4, 5.2 Hz, 1H), 3.77 (dd, J = 7.9, 2.6 Hz, 1H), 3.45 (d, J = 2.8 Hz, 1H), 3.41−3.32 (m, 1H), 2.87 (dt, J = 19.5, 2.5 Hz, 1H), 2.44 (dt, J = 19.4, 2.4 Hz, 1H), 1.26 (s, 3H). ^{13}C NMR (125 MHz): 213.8, 170.4, 163.8, 134.9, 132.7, 126.4, 75.4, 68.5, 49.9, 42.0, 41.1, 20.8 ppm. HRMS-ESI$^+$ (m/z) calcd [M + H]$^+$ for $C_{12}H_{14}O_4$: 223.0965. Found: 223.0963.

Rac-(R)-((R)-2-((tert-Butyldimethylsilyl)oxy)-1-methylcyclopent-2-en-1-yl)((S)-4-methylene-5-oxotetrahydrofuran-3-yl)methyl 4-Bromobenzoate. Compound **10b** (0.150 g, 0.443 mmol) was dissolved in DCM (4 mL). Next, 4-DMAP (0.325 g, 2.66 mmol) and 4-bromobenzoic acid (0.445 g, 2.22 mmol) were added, followed by DCC (0.457 g, 2.22 mmol). The reaction was heated to 40 °C for 16 h. The reaction was allowed to cool to RT and quenched with H_2O (5 mL). The mixture was extracted with DCM (20 mL, 3×). The organic layer was dried over Na_2SO_4 and concentrated *in vacuo*. The crude reaction product was SiO_2 purified with EtOAc (0−20%) in hexanes. The reaction afforded 0.180 g (99% yield) of a white solid. ^{1}H NMR (500 MHz): 7.89−7.82 (m, 2H), 7.63−7.56 (m, 2H), 6.12 (d, J = 2.5 Hz, 1H), 5.51 (d, J = 2.1 Hz, 1H), 5.11 (d, J = 7.5 Hz, 1H), 4.71 (t, J = 2.3 Hz, 1H), 4.46 (dd, J = 9.5, 3.8 Hz, 1H), 4.34 (dd, J = 9.5, 7.9 Hz, 1H), 3.50−3.41 (m, 1H), 2.38−2.21 (m, 3H), 1.84−1.74 (m, 1H), 1.14 (s, 3H), 0.96 (s, 9H), 0.23 (s, 3H), 0.19 (s, 3H) ppm. ^{13}C NMR (125 MHz): 170.1, 165.1, 155.8, 134.9, 132.0, 131.0, 128.7, 128.5, 125.2, 102.8, 79.5, 69.7, 51.5, 40.3, 30.5, 26.1, 25.7, 24.3, 18.1, 4.4, 5.4, impurity at 53.4 ppm. HRMS-ESI$^+$ (m/z) calcd [M + H]$^+$ for $C_{25}H_{33}BrO_5Si$: 521.1353. Found: 521.1331.

*Rac-(R)-((R)-1-Methyl-2-oxocyclopentyl)((S)-4-methylene-5-oxo-tetrahydrofuran-3-yl)methyl 4-Bromobenzoate (**11**).* The 4-bromo benzoate silyl enol ether (0.180 g, 0.035 mmol) from the previous reaction was dissolved in DCM (2 mL), and TFA (200 μL) was added to the reaction at RT. The reaction was stirred for 1 h, then quenched with aqueous $NaHCO_3$ (saturated, 10 mL) and extracted with DCM (10 mL, 3×). The organic layer was dried over Na_2SO_4 and concentrated *in vacuo*. The crude product was SiO_2 purified with EtOAc (0−40%) in hexanes to afford a white solid (0.100 g, 53% yield). ^{1}H NMR (500 MHz): 7.83−74 (m, 2H), 7.62−7.54 (m, 2H), 6.14 (d, J = 2.4 Hz, 1H), 5.53 (d, J = 1.7 Hz, 1H), 5.19 (d, J = 6.7 Hz, 1H), 4.47−4.35 (m, 2H), 3.87−3.81 (m, 1H), 2.52−2.42 (m, 1H), 2.33−2.21 (m, 1H), 2.15−2.07 (m, 1H), 2.05−1.88 (m, 3H), 1.17 (s, 3H) ppm. ^{13}C NMR (125 MHz): 220.0, 169.7, 164.8, 134.2, 132.1, 131.0, 128.9, 128.1, 126.0, 78.5, 69.8, 51.4, 39.9, 38.8, 34.2, 20.2, 18.6 ppm. HRMS-ESI$^+$ (m/z) calcd [M + H]$^+$ for $C_{19}H_{19}BrO_5$: 407.0489. Found: 407.0471.

Cell Culture. All cell lines were maintained in a humidified 5% CO_2 environment at 37 °C in tissue culture flasks (Corning) under normoxic conditions. Adherent cells were dissociated using Trypsin-EDTA solution (0.25%, Gibco). A549-NF-κB luciferase cells were cultured as described previously.[62] HeLa were cultured in MEM media (Cellgro) supplemented with 10% FBS (Gibco), penicillin (100 IU/mL, ATCC), and streptomycin (100 μg/mL, ATCC).

A549-Luciferase NF-κB reporter assay. The NF-κB-luciferase assay in stably transfected A549 cells was conducted according to a previously described protocol.[62]

Labeling in HeLa Cell Culture. HeLa cells were grown to 90% confluency in a 75 cm^2 culture flask. The culture flasks were dosed with the respective probe concentrations or a DMSO control and incubated for 1 h at 37 °C under normoxic conditions. The cells were detached with nonenzymatic cell dissociation solution (Life Technologies) and washed with cold 1× PBS buffer (10 mL, 3×). The cells were pelleted after each suspension for 5 min at 1000 rpm. After the last wash, the cells were suspended in cold 1× PBS buffer (1 mL) containing Complete EDTA-Free Protease Cocktail (Promega). The cells were lysed *via* sonication with a Vibra Cell VCX 750 (750 W, 20 kHz, 120 V) at 40% power for 30 s, while on ice. The lysates were stored at −80 °C until further use.

Lysate was allowed to thaw and kept on ice. The protein concentration was measured *via* BCA analysis (Pierce BCA Protein Assay Kit, Thermo Scientific), and all lysates were normalized to the sample with the lowest concentration. Click reagents were added to each sample (1 μL $CuSO_4$, 100 mM stock in ddH_2O; 1 μL TBTA, 20 mM stock in DMSO; 0.5 μL TAMRA-N_3,[68] 40 mM stock in DMSO; 2 μL TCEP, 100 mM in ddH_2O) and allowed to react for 3 h at RT. LDS 4× sample buffer (8 μL, NuPAGE) and 10× sample reducing agent (2 μL, NuPAGE) were then added to each sample and heated to 90 °C for 5 min before being pipetted into a 15-well NuPAGE Novex 4−12% polyacrylamide bis-tris gel and separated with electrophoresis (180 V, 54 min) in NuPAGE MES SDS running buffer (1×). Gels were imaged using a TyphoonFLA7000 gel imager (General Electric). Images were analyzed using ImageQuant TL v7.0 software.

Pulldown Experiments. HeLa cells were allowed to grow to 90% confluency in a 150 cm^2 flask under normoxic conditions at 37 °C in a humidified CO_2 incubator. The medium was replaced with 20 mL of fresh medium, and the competition compounds **6a** and **6b** or a DMSO control was dosed to achieve the final concentration (50 μM, DMSO concentration <0.05%) in each flask and incubated for 20 min. Alkyne probes **1a** or **1b** were dosed at 50 μM and incubated for an additional 30 min. After incubation, the medium was removed, and the cells were washed with cold 1× PBS (10 mL). The cells were then dissociated from the flask using nonenzymatic dissociation media (4 mL, Life Technologies). The cells were collected in 1× PBS (8 mL) and centrifuged (1000 rpm, 5 min, RT) in a conical tube. The cells were washed with cold 1× PBS (10 mL) and centrifuged again. The cells were then taken up in 1× PBS (2.5 mL) containing protease inhibitor (Complete EDTA-free protease inhibitor cocktail, Life Technologies). The cells were lysed *via* sonication with a Vibra Cell VCX 750 (750 W,

DOI: 10.1021/acschembio.6b00751
ACS Chem. Biol. XXXX, XXX, XXX−XXX

20 kHz, 120 V) at 40% power for 30 s, while on ice. The lysates were stored at −80 °C until further use.

After thawing, the samples were centrifuged at 4000 rpm for 20 min at 0 °C to clear the lysate. The samples were transferred to clean conical tubes, and 200 μL of 10 w/v% SDS in ddH_2O were added and heated to 65 °C for 10 min. The protein concentration of each sample was measured *via* BCA analysis (Pierce BCA Protein Assay Kit, Thermo Scientific), and all lysates were normalized to the sample with the lowest concentration (between 1.0 to 1.6 mg mL^{-1}). Click reagents were added (10 μL $CuSO_4$, 100 mM stock in ddH_2O; 20 μL TBTA, 20 mM stock in DMSO; 20 μL Biotin-N_3 [Sigma-Aldrich 762024; CAS: 875770−34−6], 20 mM stock in DMSO; 10 μL TCEP, 100 mM in ddH_2O) and allowed to react for 3 h at RT. After incubation, 15 μL of each sample was collected and saved for the input lysate control.

The samples were then separated on a monomeric avidin column according to the manufacturer's instructions (Pierce) at 4 °C. The biotinylated samples were eluted using the regeneration buffer (0.1 M HCl glycine buffer, pH 2.8). *Note: biotinylated samples did not elute using the elution biotin buffer*. After the samples were collected, they were concentrated using a 10 kDa molecular weight cutoff filter (Amicon), ddH_2O (20 mL, 2×) was added, centrifuged, and finally the samples were concentrated to ∼500 μL. The samples were collected and concentrated to dryness in a SpeedVac for 10 h at RT. These samples were then dissolved in ddH_2O (20 μL), 10× reducing agent (2 μL, NuPAGE), and 4× sample buffer (10 μL, NuPAGE) and vortexed. Sample buffer and reducing agent were added to the input lysates in the same fashion, and all samples were heated to 90 °C for 5 min before pipetting 15 μL of each sample into a 15-well NuPAGE Novex 4−12% polyacrylamide bis-tris gel and separated with electrophoresis (180 V, 54 min) in NuPAGE MES SDS running buffer (1×). The samples were separated and transferred (30 V, 1 h, RT) in 1× TBE buffer to a PVDF membrane (Immobilon-FL) for Western blot analysis. Membranes were incubated with the respective primary antibodies (p65, Santa Cruz, sc-372; p50, Santa Cruz sc-8414; IκBα, Santa Cruz sc-371; IKKα/β, Santa Cruz sc-7607) with a 1:1000 dilution in 0.5% nonfat milk (BioRad) in 1× PBS (10 mL) overnight at 4 °C. Secondary HRP-conjugated antibodies (antirabbit poly-HRP, Pierce cat # 32260; secondary antimouse, Novex HRP cat # A16072) were added to 0.5% nonfat milk (BioRad) in 1× PBS (10 mL) at a 1:5000 dilution for 1 h at RT. Membranes were washed in ddH_2O between each incubation (30 mL for 1 min, 5×). Super Signal West Dura Extended Duration Luminol/Enhancer Solution (1 mL) and Stable Peroxide Buffer (1 mL) were added to the top of the membrane and imaged with a Li-COR Odyssey Fc imaging system. After each antibody was detected, the membrane was stripped with Restore PLUS Western Blot Stripping Buffer (Thermo), washed with ddH_2O for 30 min, and blocked overnight at 4 °C in 0.5% w/v nonfat dry milk (BioRad) in 1× PBS before incubating with the next antibody.

Labeling Recombinant Human p65. Recombinant human p65 in buffer (this clone has five point mutations compared to the p65 sequence listed under accession no. AAA36408: L159V, P180S, F309S, A439V and V462M; Active Motif) was placed in an Eppendorf tube (3 μL, 100 ng/μL) with ddH_2O (6 μL) and incubated with 100 μM of helenalin, **6a**, **6b**, **1a**, or **1b** for 1 h at RT. LDS 4× sample buffer (4 μL, NuPAGE) and 10× sample reducing agent (1 μL, NuPAGE) were then added to each sample and heated to 90 °C for 5 min before being pipetted into a 15-well NuPAGE Novex 4−12% polyacrylamide bis-tris gel and run into the top of the gel with electrophoresis (180 V, 5 min) in NuPAGE MES SDS running buffer (1×). The top of each well where the protein was located was excised and placed into an Eppendorf tube.

The gel pieces were then processed by in-gel trypsin digestion according to a previously reported protocol.[69,70] The peptides were desalted using a P10 C_{18} Zip-Tip (Millipore). Samples were dried with a SpeedVac for 3 h at RT, and the dried peptides were dissolved in 95:5 H_2O/MeCN 0.1% formic acid solution (12 μL) for HPLC- ESI^+-MS/MS analysis.

HPLC-ESI^+-MS/MS analyses of tryptic peptides were conducted using an Orbitrap Fusion mass spectrometer (Thermo Scientific) equipped with a Dionex Ultimate UHPLC pump (Thermo Scientific), a nanospray source, and Xcalibur 3.0.63 software for instrument control. Peptide mixtures were directly injected onto a nanoHPLC column (75 μm i.d., 10 cm packed bed, 15 μm orifice) created by hand packing a commercially purchased fused-silica emitter (New Objective) with Zorbax SB-C18 5 μm separation media (Agilent). The gradient program started from 0 to 17 min at 2% MeCN/H_2O (1% formic acid) with a flow rate of 3 μL/min, followed by a linear increase to 30% MeCN/H_2O (1% formic acid) from 17 to 80 min, followed by a linear increase to 80% MeCN/H_2O (1% formic acid) from 80 to 91 min. Finally, the column was equilibrated with 2% MeCN/H_2O (1% formic acid) from 91 to 99 min with a flow rate of 9 μL/min. Liquid chromatography was carried out at an ambient temperature. The mass spectrometer was calibrated prior to each analysis, and the spray voltage was adjusted to ensure a stable spray. The MS tune parameters were as follows: spray voltage of 2.460 kV, capillary temperature of 300 °C, and an S-lens RF level of 60%. MS/MS spectra were collected using simultaneous data-dependent scanning and target mass analysis, in which one full scan mass spectrum is acquired in the Orbitrap detector (R = 120 000, scan range 320−2000 m/z), followed by a target list analyzing masses corresponding to expected theoretical probe-peptide adducts (343.6443, 489.2235, 640.8083, 770.8567, 229.4320, 326.4848, 427.5413, 514.2402, 923.7783, 693.0855, 569.7730, 383.6574, 529.2365, 353.1601, 680.8214, 454.2167 m/z), followed by 12 data-dependent MS/MS spectra acquired with the Orbitrap detector (R = 15 000) with charge states 2−7, dynamic exclusion after one detection for 20 s, an intensity threshold of 5.0×10^4, and a mass tolerance of 10.00 ppm. The method uses an isolation width of 1.6 m/z, maximum injection time of 150 ms, 40% HCD collision energy, and 1 AGC microscan. Spectral data were analyzed using the Proteomic Discoverer software package (v1.4.0.288, ThermoFisher). Data were processed using the SEQUEST v.27 algorithm.[71] Peptide spectra were searched against the UniProt Human Protein Database. Helenalin (+262.1205 Da), **6a** and **6b** (+222.0892), **1a** and **1b** (+302.3260 Da), and/or cysteine carboxamidomethylation (+57.0215 Da) were set as a dynamic modification. Precursor mass tolerance was set to 10 ppm within the calculated mass, and fragment ion mass tolerance was set to 10 mmu of their monoisotopic mass. Probe-peptide adducts found using the Proteome Discoverer software were further scrutinized by manually extracting the mass using the Xcalibur software from the total ion chromatogram. The MS^2 fragmentation data were analyzed manually to confirm the identity of probe-peptide adducts.

■ ASSOCIATED CONTENT

Supporting Information

The Supporting Information is available free of charge on the ACS Publications website at DOI: 10.1021/acschembio.6b00751.

NMR and analytical HPLC characterization of synthesized compounds, determination of enantiomeric ratio of **6a** and **6b**, molecular modeling of probe compounds, peptide-probe MS^2 fragmentation data, and crystallographic information (PDF)

Crystallographic information for **11** (CIF)

■ AUTHOR INFORMATION

Corresponding Author

*E-mail: daharki@umn.edu.

ORCID

Daniel A. Harki: 0000-0001-5950-931X

Notes

The authors declare no competing financial interest.

DOI: 10.1021/acschembio.6b00751
ACS Chem. Biol. XXXX, XXX, XXX−XXX

ACKNOWLEDGMENTS

The work was generously supported by the University of Minnesota (Academic Health Center Seed Grant #2010.01), The V Foundation for Cancer Research (V Scholar Award to D. A. Harki), Hyundai Hope on Wheels (Hope Grant), and the NIH (R21-CA194661). J. C. Widen acknowledges the University of Minnesota, College of Pharmacy for a Bighley Graduate Fellowship. Mass spectrometry was performed at the Analytical Biochemistry Core Facility of the Masonic Cancer Center, which is supported by the NIH (P30-CA77598 and S10 RR-024618). We gratefully acknowledge V. G. Young, Jr. (University of Minnesota, Department of Chemistry, X-ray Crystallographic Laboratory) for solving the structure of **11** and funding from the NSF/MRI (#1229400) and the University of Minnesota for the purchase of the Bruker-AXS D8 Venture diffractometer. The Minnesota Supercomputing Institute (MSI) at the University of Minnesota is acknowledged for molecular modeling resources.

ABREVIATIONS

Cys, cysteine; IBX, 2-Iodoxybenzoic acid; DMSO, dimethyl sulfoxide; PCC, pyridinium chlorochromate; DCC, N,N′-dicyclohexylcarbodiimide; RT, room temperature; PhH, benzene; LDA, lithium diisopropylamine; LiHMDS, Lithium bis(trimethylsilyl)amide; 4-DMAP, 4-dimethylaminopyridine; TBSCl, *tert*-butyldimethylsilyl chloride; atm, atmosphere; sec, seconds; min, minutes; dr, diastereomeric ratio; er, enantiomeric ratio; sat, saturated; aq, aqueous; GC, gas chromatography; TFA, trifluoroacetic acid; LC-MS, liquid chromatography−mass spectrometry; SDS-PAGE, sodium dodecyl sulfate-polyacrylamide gel electrophoresis; (S)-MTPA, (S)-α-Methoxy-α-trifluoromethylphenylacetic acid; TMS, tetramethylsilane; EtOAc, ethyl acetate; EDTA, Ethylenediaminetetraacetic acid; ESI, electrospray ionization; HPLC, high-performance liquid chromatography; UHPLC, ultra high-performance liquid chromatography; TBE, tris boric acid EDTA buffer; ddH_2O, distilled and deionized water; HRMS-ESI, high resolution mass spectrometry-electrospray ionization; PVDF, polyvinylidene difluoride

REFERENCES

(1) Xiao, G., and Fu, J. (2011) NF-κB and Cancer: a Paradigm of Yin-Yang. *Am. J. Cancer Res. 1*, 192−221.

(2) Aggarwal, B. B. (2004) Nuclear factor-κB the enemy within. *Cancer Cell 6*, 203−208.

(3) Huxford, T., and Ghosh, G. (2009) A structural guide to proteins of the NF-κB signaling module. *Cold Spring Harbor Perspect. Biol. 1*, a000075.

(4) Hayden, M. S., and Ghosh, S. (2008) Shared principles in NF-κB signaling. *Cell 132*, 344−362.

(5) Greten, F. R., and Karin, M. (2004) The IKK/NF-κB activation pathway-a target for prevention and treatment of cancer. *Cancer Lett. 206*, 193−199.

(6) Pande, V., Sousa, S. F., and Ramos, M. J. (2009) Direct covalent modification as a strategy to inhibit nuclear factor-κB. *Curr. Med. Chem. 16*, 4261−4273.

(7) Wang, W., Nag, S. A., and Zhang, R. (2015) Targeting the NF-κB signaling pathways for breast cancer prevention and therapy. *Curr. Med. Chem. 22*, 264−289.

(8) Karin, M., Yamamoto, Y., and Wang, Q. M. (2004) The IKK NF-κB system: A treasure trove for drug development. *Nat. Rev. Drug Discovery 3*, 17−26.

(9) Gilmore, T. D., and Herscovitch, M. (2006) Inhibitors of NF-κB signaling: 785 and counting. *Oncogene 25*, 6887−6899.

(10) Gupta, S. C., Sundaram, C., Reuter, S., and Aggarwal, B. B. (2010) Inhibiting NF-κB activation by small molecules as a therapeutic strategy. *Biochim. Biophys. Acta, Gene Regul. Mech. 1799*, 775−787.

(11) Raskatov, J. A., Meier, J. L., Puckett, J. W., Yang, F., Ramakrishnan, P., and Dervan, P. B. (2012) Modulation of NF-κB-dependent gene transcription using programmable DNA minor groove binders. *Proc. Natl. Acad. Sci. U. S. A. 109*, 1023−1028.

(12) Kojima, T., Wang, X., Fujiwara, K., Osaka, S., Yoshida, Y., Osaka, E., Taniguchi, M., Ueno, T., Fukuda, N., Soma, M., Tokuhashi, Y., and Nagase, H. (2014) Inhibition of human osteosarcoma cell migration and invasion by a gene silencer, pyrrole-imidazole polyamide, targeted at the human MMP9 NF-κB binding site. *Biol. Pharm. Bull. 37*, 1460−1465.

(13) Wurtz, N. R., Pomerantz, J. L., Baltimore, D., and Dervan, P. B. (2002) Inhibition of DNA binding by NF-κB with pyrrole-imidazole polyamides. *Biochemistry 41*, 7604−7609.

(14) Chenoweth, D. M., Poposki, J. A., Marques, M. A., and Dervan, P. B. (2007) Programmable oligomers targeting 5′-GGGG-3′ in the minor groove of DNA and NF-κB binding inhibition. *Bioorg. Med. Chem. 15*, 759−770.

(15) Yang, F., Nickols, N. G., Li, B. C., Szablowski, J. O., Hamilton, S. R., Meier, J. L., Wang, C. M., and Dervan, P. B. (2013) Animal toxicity of hairpin pyrrole-imidazole polyamides varies with the turn unit. *J. Med. Chem. 56*, 7449−7457.

(16) Koehler, A. N. (2010) A complex task? Direct modulation of transcription factors with small molecules. *Curr. Opin. Chem. Biol. 14*, 331−340.

(17) Berg, T. (2008) Inhibition of transcription factors with small organic molecules. *Curr. Opin. Chem. Biol. 12*, 464−471.

(18) Merfort, I. (2011) Perspectives on sesquiterpene lactones in inflammation and cancer. *Curr. Drug Targets 12*, 1560−1573.

(19) Siedle, B., Garcia-Pineres, A. J., Murillo, R., Schulte-Monting, J., Castro, V., Rungeler, P., Klaas, C. A., Da Costa, F. B., Kisiel, W., and Merfort, I. (2004) Quantitative structure-activity relationship of sesquiterpene lactones as inhibitors of the transcription factor NF-κB. *J. Med. Chem. 47*, 6042−6054.

(20) Adams, R., and Herz, W. (1949) Helenalin. I. Isolation and Properties. *J. Am. Chem. Soc. 71*, 2546−2551.

(21) Kos, O., Lindenmeyer, M. T., Tubaro, A., Sosa, S., and Merfort, I. (2005) New sesquiterpene lactones from Arnica tincture prepared from fresh flowerheads of Arnica montana. *Planta Med. 71*, 1044−1052.

(22) Pettit, G. R., Budzinski, J. C., Cragg, G. M., Brown, P., and Johnston, L. D. (1974) Antineoplastic Agents. 34. Helenium-Autumnale-L. *J. Med. Chem. 17*, 1013−1016.

(23) Lamson, P. D. (1913) On the Pharmacological Action of Helenin, the Active Principle of Helenium Autumnale. *J. Pharmacol. Exp. Ther. 4*, 471−489.

(24) Kitson, R. R., Millemaggi, A., and Taylor, R. J. (2009) The Renaissance of α-methylene-γ-butyrolactones: New Synthetic Approaches. *Angew. Chem., Int. Ed. 48*, 9426−9451.

(25) Lee, K. H., Ibuka, T., Mar, E. C., and Hall, I. H. (1978) Antitumor agents. 31. Helenalin sym-dimethylethylenediamine reaction products and related derivatives. *J. Med. Chem. 21*, 698−701.

(26) Lee, K. H., Huang, E. S., and Furukawa, H. (1972) Antitumor Agents. 3. Synthesis and Cytotox Activity of Helenalin Amine Adducts and Related Derivatives. *J. Med. Chem. 15*, 609−611.

(27) Lee, K. H., Kim, S. H., Furukawa, H., Piantadosi, C., and Huang, E. S. (1975) Antitumor Agents. 11. Synthesis and Cytotox Activity of Epoxides of Helenalin Related Derivatives. *J. Med. Chem. 18*, 59−63.

(28) Grippo, A. A., Hall, I. H., Kiyokawa, H., Muraoka, O., Shen, Y. C., and Lee, K. H. (1992) The cytotoxicity of helenalin, its mono and difunctional esters, and related sesquiterpene lactones in murine and human tumor cells. *Drug Des. Discovery 8*, 191−206.

(29) Hall, I. H., Lee, K. H., Mar, E. C., Starnes, C. O., and Waddell, T. G. (1977) Antitumor Agents. 21. A Proposed Mechanism for Inhibition of Cancer Growth by Tenulin and Helenalin and Related Cyclopentenones. *J. Med. Chem. 20*, 333−337.

DOI: 10.1021/acschembio.6b00751
ACS Chem. Biol. XXXX, XXX, XXX−XXX

(30) Schmidt, T. J. (1997) Helenanolide-type sesquiterpene lactones–III. Rates and stereochemistry in the reaction of helenalin and related helenanolides with sulfhydryl containing biomolecules. *Bioorg. Med. Chem. 5*, 645−653.

(31) Lyss, G., Knorre, A., Schmidt, T. J., Pahl, H. L., and Merfort, I. (1998) The Anti-inflammatory Sesquiterpene Lactone Helenalin Inhibits the Transcription Factor NF-κB by Directly Targeting p65. *J. Biol. Chem. 273*, 33508−33516.

(32) Buchele, B., Zugmaier, W., Lunov, O., Syrovets, T., Merfort, I., and Simmet, T. (2010) Surface Plasmon Resonance Analysis of Nuclear Factor-κB Protein Interactions with the Sesquiterpene Lactone Helenalin. *Anal. Biochem. 401*, 30−37.

(33) Chen, F. E., Huang, D. B., Chen, Y. Q., and Ghosh, G. (1998) Crystal Structure of p50/p65 Heterodimer of Transcription Factor NF-κB Bound to DNA. *Nature 391*, 410−413.

(34) Garcia-Pineres, A. J., Castro, V., Mora, G., Schmidt, T. J., Strunck, E., Pahl, H. L., and Merfort, I. (2001) Cysteine 38 in p65/NF-κB Plays a Crucial Role in DNA Binding Inhibition by Sesquiterpene Lactones. *J. Biol. Chem. 276*, 39713−39720.

(35) Cys38 and Cys120 of p65 are spatially separated by 7.7 Å in PDB 1VKX. This distance is similar to spatial separation of the two electrophilic carbons in helenalin from two published crystal structures and a computationally minimized structure. See Supporting Information for additional details.

(36) Rungeler, P., Castro, V., Mora, G., Goren, N., Vichnewski, W., Pahl, H. L., Merfort, I., and Schmidt, T. J. (1999) Inhibition of transcription factor NF-κB by sesquiterpene lactones: a proposed molecular mechanism of action. *Bioorg. Med. Chem. 7*, 2343−2352.

(37) Kastrati, I., Siklos, M. I., Calderon-Gierszal, E. L., El-Shennawy, L., Georgieva, G., Thayer, E. N., Thatcher, G. R., and Frasor, J. (2016) Dimethyl Fumarate Inhibits the Nuclear Factor κB Pathway in Breast Cancer Cells by Covalent Modification of p65 Protein. *J. Biol. Chem. 291*, 3639−3647.

(38) Han, Y., Englert, J. A., Yang, R., Delude, R. L., and Fink, M. P. (2005) Ethyl Pyruvate Inhibits Nuclear Factor-κB-dependent Signaling by Directly Targeting p65. *J. Pharmacol. Exp. Ther. 312*, 1097−1105.

(39) Sethi, G., Ahn, K. S., and Aggarwal, B. B. (2008) Targeting Nuclear factor-κB Activation Pathway by Thymoquinone: Role in Suppression of Antiapoptotic Gene Products and Enhancement of Apoptosis. *Mol. Cancer Res. 6*, 1059−1070.

(40) Liang, M. C., Bardhan, S., Pace, E. A., Rosman, D., Beutler, J. A., Porco, J. A., Jr., and Gilmore, T. D. (2006) Inhibition of Transcription Factor NF-κB Signaling Proteins IKKβ and p65 Through Specific Cysteine Residues by Epoxyquinone A Monomer: Correlation with its Anti-cancer Cell Growth Activity. *Biochem. Pharmacol. 71*, 634−645.

(41) Rana, S., Blowers, E. C., Tebbe, C., Contreras, J. I., Radhakrishnan, P., Kizhake, S., Zhou, T., Rajule, R. N., Arnst, J. L., Munkarah, A. R., Rattan, R., and Natarajan, A. (2016) Isatin Derived Spirocyclic Analogues with α-methylene-γ-butyrolactone as Anticancer Agents: A Structure-Activity Relationship Study. *J. Med. Chem. 59*, 5121−5127.

(42) Yamamoto, M., Horie, R., Takeiri, M., Kozawa, I., and Umezawa, K. (2008) Inactivation of NF-κB Components by Covalent Binding of (−)-dehydroxymethylepoxyquinomicin to Specific Cysteine Residues. *J. Med. Chem. 51*, 5780−5788.

(43) Deny, L. J., Traboulsi, H., Cantin, A. M., Marsault, E., Richter, M. V., and Belanger, G. (2016) Bis-Michael Acceptors as Novel Probes to Study the Keap1/Nrf2/ARE Pathway. *J. Med. Chem. 59*, 9431−9442.

(44) Grieco, P. A., Majetich, G. F., and Ohfune, Y. (1982) Pseudoguaianolides. 1. Stereospecific Total Synthesis of the Ambrosanolides dl-Ambrosin and dl-Damsin. *J. Am. Chem. Soc. 104*, 4226−4233.

(45) Grieco, P. A., Ohfune, Y., Majetich, G. F., and Wang, C. L. J. (1982) Pseudoguaianolides 0.2. Stereocontrolled Total Synthesis of the Helenanolide dl-Helenalin. *J. Am. Chem. Soc. 104*, 4233−4240.

(46) Ohfune, Y., Grieco, P. A., Wang, C. L. J., and Majetich, G. (1978) Stereospecific Total Synthesis of dl-Helenalin - General Route to Helenanolides and Ambrosanolides. *J. Am. Chem. Soc. 100*, 5946−5948.

(47) Roberts, M. R., and Schlessinger, R. H. (1979) Total Synthesis of dl-Helenalin. *J. Am. Chem. Soc. 101*, 7626−7627.

(48) Watson, W. H., and Kashyap, R. P. (1990) The Structures of 2 Sesquiterpene Lactones. *Acta Crystallogr., Sect. C: Cryst. Struct. Commun. 46*, 1524−1528.

(49) Fronczek, F. R., Ober, A. G., and Fischer, N. H. (1987) Helenalin, a Pseudoguaianolide from Helenium-Amarum. *Acta Crystallogr., Sect. C: Cryst. Struct. Commun. 43*, 358−360.

(50) Hodgson, D. M., Talbot, E. P. A., and Clark, B. P. (2011) Stereoselective Synthesis of β-(hydroxymethylaryl/alkyl)-α-methylene-γ-butyrolactones. *Org. Lett. 13*, 2594−2597.

(51) Ramachandran, P. V., Chen, G. M., and Brown, H. C. (1996) Chiral Synthesis Via Organoboranes. 42. Selective Reductions. 57. Efficient Kinetic Resolution of Representative α-tertiary Ketones with B-chlorodiisopinocampheylborane. *J. Org. Chem. 61*, 88−94.

(52) Sato, K. S. S., Kojima, Y., and Suzuki, S. (1967) A New Synthesis of 3-Methylcyclopent-2-en-2-ol-1-one. *J. Org. Chem. 32*, 339−341.

(53) Lee, K. H., Mar, E. C., Okamoto, M., and Hall, I. H. (1978) Antitumor Agents 32. Synthesis and Antitumor Activity of Cyclopentenone Derivatives Related to Helenalin. *J. Med. Chem. 21*, 819−822.

(54) Nicolaou, K. C., Montagnon, T., Baran, P. S., and Zhong, Y. L. (2002) Iodine(V) Reagents in Organic Synthesis. Part 4. O-iodoxybenzoic acid as a Chemospecific Tool for Single Electron Transfer-based Oxidation Processes. *J. Am. Chem. Soc. 124*, 2245−2258.

(55) Fuchs, M., Schober, M., Orthaber, A., and Faber, K. (2013) Asymmetric Synthesis of β-Substituted α-methylenebutyrolactones *via* TRIP-Catalyzed Allylation: Mechanistic Studies and Application to the Synthesis of (S)-(−)-Hydroxymatairesinol. *Adv. Synth. Catal. 355*, 2499−2505.

(56) Ando, K., Takemasa, Y., Tomioka, K., and Koga, K. (1993) Stereoselective reactions. XXI. Asymmetric alkylation of α-alkyl β-keto-esters to α,α-dialkyl β-keto-esters having either (R)-chiral or (S)-chiral quaternary center depending on the solvent system. *Tetrahedron 49*, 1579−1588.

(57) Fukuyama, Y., Matsumoto, K., Tonoi, Y., Yokoyama, R., Takahashi, H., Minami, H., Okazaki, H., and Mitsumoto, Y. (2001) Total syntheses of neuroprotective mastigophorenes A and B. *Tetrahedron 57*, 7127−7135.

(58) Fukuyama, Y., Kiriyama, Y., and Kodama, M. (1996) Total synthesis of herbertenediol, an isocuparane sesquiterpene isolated from liverworts. *Tetrahedron Lett. 37*, 1261−1264.

(59) Lee, J. N., Oya, S., and Snyder, J. K. (1991) Asymmetric Oxidation of β-Ketoesters with Benzoyl Peroxide - Enantioselective Formation of Protected Tertiary Alcohols. *Tetrahedron Lett. 32*, 5899−5902.

(60) Ito, Y., Hirao, T., and Saegusa, T. (1978) Synthesis of α,β-Unsaturated Carbonyl-Compounds by Palladium(II)-Catalyzed Dehydrosilylation of Silyl Enol Ethers. *J. Org. Chem. 43*, 1011−1013.

(61) Larock, R. C., Hightower, T. R., Kraus, G. A., Hahn, P., and Zheng, D. (1995) A Simple, Effective, New, Palladium-Catalyzed Conversion of Enol Silanes to Enones and Enals. *Tetrahedron Lett. 36*, 2423−2426.

(62) Hexum, J. K., Tello-Aburto, R., Struntz, N. B., Harned, A. M., and Harki, D. A. (2012) Bicyclic Cyclohexenones as Inhibitors of NF-κB Signaling. *ACS Med. Chem. Lett. 3*, 459−464.

(63) Rostovtsev, V. V., Green, L. G., Fokin, V. V., and Sharpless, K. B. (2002) A stepwise huisgen cycloaddition process: copper(I)-catalyzed regioselective "ligation" of azides and terminal alkynes. *Angew. Chem., Int. Ed. 41*, 2596−2599.

(64) Frigerio, M., Santagostino, M., and Sputore, S. (1999) A user-friendly entry to 2-iodoxybenzoic acid (IBX). *J. Org. Chem. 64*, 4537−4538.

(65) Kozawa, I., Akashi, Y., Takiguchi, K., Sasaki, D., Sawamoto, D., Takao, K., and Tadano, K. (2007) Stereoselective double alkylation of the acetoacetate ester α-carbon on a D-glucose-derived template:

DOI: 10.1021/acschembio.6b00751
ACS Chem. Biol. XXXX, XXX, XXX−XXX

Application to the synthesis of enantiopure cycloalkenones bearing an asymmetric quaternary carbon. *Synlett 2007*, 399−402.

(66) Kato, K., Suzuki, H., Tanaka, H., Miyasaka, T., Baba, M., Yamaguchi, K., and Akita, H. (1999) Stereoselective Synthesis of 4′-α-alkylcarbovir Derivatives Based on an Asymmetric Synthesis or Chemoenzymatic Procedure. *Chem. Pharm. Bull. 47*, 1256−1264.

(67) Kumar, R., Rej, R. K., Halder, J., Mandal, H., and Nanda, S. (2016) Enantiopure Hydroxymethylated Cycloalkenols as Privileged Small Molecular Multifunctional Scaffolds for the Asymmetric Synthesis of Carbocycles. *Tetrahedron: Asymmetry 27*, 498−512.

(68) Friscourt, F., Fahrni, C. J., and Boons, G. J. (2012) A Fluorogenic Probe for the Catalyst-free Detection of Azide-tagged Molecules. *J. Am. Chem. Soc. 134*, 18809−18815.

(69) Shevchenko, A., Wilm, M., Vorm, O., and Mann, M. (1996) Mass Spectrometric Sequencing of Proteins from Silver Stained Polyacrylamide Gels. *Anal. Chem. 68*, 850−858.

(70) Shevchenko, A., Tomas, H., Havlis, J., Olsen, J. V., and Mann, M. (2006) In-gel Digestion for Mass Spectrometric Characterization of Proteins and Proteomes. *Nature Prot. 1*, 2856−2860.

(71) Yates, J. R., 3rd, Eng, J. K., and McCormack, A. L. (1995) Mining Genomes: Correlating Tandem Mass Spectra of Modified and Unmodified Peptides to Sequences in Nucleotide Databases. *Anal. Chem. 67*, 3202−3210.

DOI: 10.1021/acschembio.6b00751
ACS Chem. Biol. XXXX, XXX, XXX−XXX